Superlattices and Microstructures, Vol. 27, No. 2/3,2000
doi:10.1006/spmi.1999.0808
Available online at http://www.idealibrary.com on IDEAL

Ballistic field-effect transistor with negative-effective-mass current carriers in the channel

Z. GRIBNIKOV, N. VAGIDOV, A. KORSHAK, V. MITIN
Department of Electrical and Computer Engineering, Wayne State University, Detroit, MI 48202, U.S.A.

(Received 9 November 1999)

We consider a ballistic field-effect transistor with channel current carriers having a negative effective mass section in their dispersion relation. Such a device is suggested as an effective generator of terahertz-range oscillations. A gate potential controls the generator regime (including oscillation frequency, amplitude, turning on and off).

Key words: ballistic transport, negative effective mass, field-effect transistor.

1. Introduction

A channel current of a sufficiently long ballistic field-effect transistor (FET) is saturated beginning with a drain potential $V = V_S = (1/3)edN_d^*$, where $N_d^* = N_d + (2V_G/ed)$ and e is the electron charge. (We assume that the FET contains a planar channel doped by ionized acceptors or donors with a concentration $N_d(\mathrm{cm}^{-2})$. Metallic gates with the same potentials V_G are placed on both sides of the channel in a distance d. A saturation current (A cm^{-1}) is determined by the expression: $I = I_S = e^2(2dN_d^{*3}/27m)^{1/2}$. The formulae for V_S and I_S are obtained for the simplest parabolic dispersion relation $\varepsilon(p) = p^2/2m$, where p is a momentum, and m is an effective mass. A more complicated model of the ballistic FET with the same dispersion relation [1, 2] leads to analogous results. As was shown in [2], stationary IV-characteristics of such ballistic FETs can be unstable in sections of increasing current ($V < V_S$) as a result of development of two-stream instability [3, 4], but they are stable in saturation sections ($V > V_S$). It is because the single stream of the traversing ballistic carriers with energy eV_S is left in the channel at the saturation regime, and the carriers, which are in equilibrium with the drain reservoir, are absent.

In this paper we are interested in the more complicated dispersion relation shown in Fig. 1. It contains a negative effective mass (NEM) section around energy $\varepsilon = \varepsilon_C$. It is known [5] that a current in this case is saturated without any gates in a certain drain potential range: $\varepsilon_C/e \le V \le \varepsilon_K/e$ (where the meaning of ε_K is understandable from Fig. 1). This saturated current is equal to $I = I_C = e\nu_C N_d$ where ν_C is a ballistic carrier velocity in a quasineutral segment (QS) of the channel: $\nu_C = (d\varepsilon/dp)$ for $p = p_C$. A carrier concentration in the QS is equal to the ionized impurity concentration, and all these carriers are the NEM carriers. Therefore, a homogeneous carrier distribution in this ballistic plasma is unstable, and terahertz electric oscillations are generated as a result of development of NEM ballistic plasma instability. An oscillation frequency exceeds 1 THz if a channel length is shorter than 0.2 μm [6, 7].

0749–6036/00/020105 + 05 $35.00/0

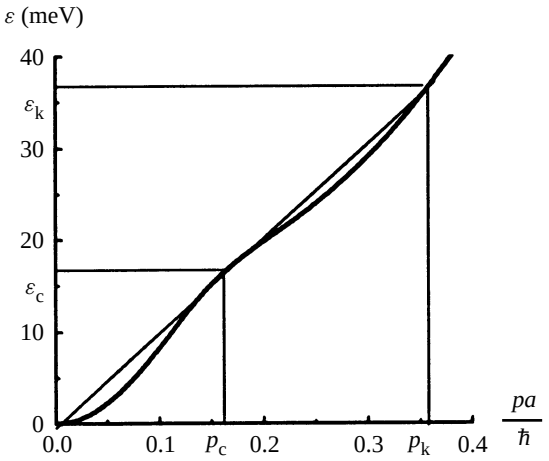

Fig. 1. Quantized hole dispersion relation $\varepsilon = \varepsilon(p)$ for the ground state in 8 nm square p-type GaAs/AlAs QW; a is a lattice constant; $\hbar$ is the Planck constant.

2. NEM ballistic FET

Here we consider a ballistic FET with the dispersion relation of channel current carriers shown in Fig. 1. The presented dispersion relation relates to quantized holes of the ground quantization subband for a square 8 nm p-type GaAs/AlAs quantum well (see details in [8]). These holes are selected here as current carriers in the channel of the calculated FET. Stationary IV-characteristics of such a device depend substantially on relation between the values of the above introduced V_S and $V_C = \varepsilon_C/e$. While a condition $V_S \ll V_C$ is satisfied, the NEM section of the dispersion relation does not influence the FET action considered above. For the opposite relation $V_C \ll V_S$ a FET behavior is presented by two saturation regimes: (1) an intermediate saturation that begins with $V = V_C$ and (2) a final saturation that begins with $V = V_S$. A saturated current for the former is determined by the formula: $I = I_C^* = ev_C N_d^*$. It can be controlled with a gate potential V_G as in the ordinary FET, but the potential of saturation V_C is determined only by a position of the NEM section in the carrier dispersion relation. Therefore, carriers in the quasineutral channel segment are NEM, and the instability of their homogeneous distribution occurs and leads to the oscillation generation. Distinction of these oscillations is that an oscillating current flows basically en route from gate to drain, and a source current is almost stationary. A gate potential V_G not only controls a stationary source current but it also turns the FET on and off the oscillatory regime. The second (final) saturation beginning with $\approx V_S (> V_K \varepsilon_K/e)$ is characterized by current $I = I_S^*$ that is determined by the same formula for I_S in which effective mass m for the small values of momentum $p < p_C$ is replaced with effective mass m^* for large $p > p_C$.

3. Numerical calculations

We confirm the above-stated qualitative arguments with the direct numerical calculations and use for this aim a more realistic FET model (Fig. 2) with a single top gate and a two-dimensional hole gas current-conducting channel. The channel connects plane p^+-source with p^+-drain and serves as a p-base of the obtained p^+pp^+-diode. A length of this base l is selected at 0.2 μm for our calculations. We assume that both the source and the drain supply the base channel with Fermi–Dirac-distributed holes having the given Fermi-energy ($\mu = 10$ meV). The channel is directly doped with ionized acceptors ($N_d = 10^{11}$ cm^{-2}). This is assumed to simplify calculations, but really to reach the ballistic transport the modulation doping by the acceptor sheets in the barriers is required instead of the direct doping. A dispersion relation of holes is shown

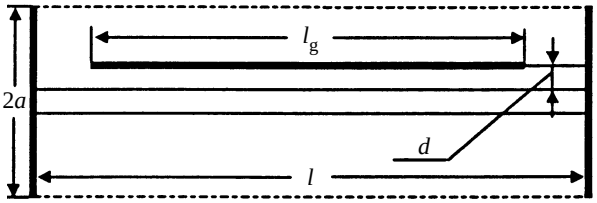

Fig. 2. Numerically modeled top-gated FET with a p-type conducting channel.

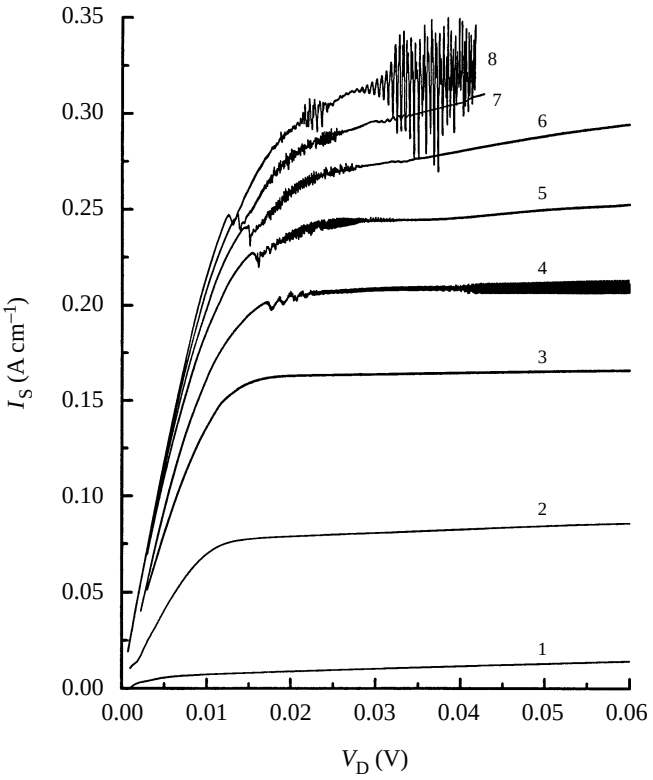

Fig. 3. Source current I_S versus drain potential V for gate potentials $V_G = 50$ mV (1), 25 mV (2), O (3), -25 mV (4), -50 mV (5), -75 mV (6), -100 mV (7), -125 mV (8). In the range 0.03–0.045 V there are large-amplitude low-frequency (≈400 GHz) source current oscillations on curve 8.

in Fig. 1. The metallic gate is placed at a distance, d, of 16 nm from the channel and it covers the channel almost entirely (excluding edge clearances at the source and the drain equal to $(l - l_g)/2 = 0.02$ μm).

A kinetic equation for one-dimensional ballistic transport of quantized holes in the channel is solved self-consistently with a two-dimensional Poisson equation in the entire space between the drain and the source planes. In the y-direction, periodicity conditions (with spatial period $2a = 0.16$ μm) are used as boundary conditions. It is shown [8] that such a period value allows us to consider parallel current-conducting channels as almost independent devices. Calculations are carried out for AlAs-barrier medium (with the dielectric constant $\kappa_D = 10.9$) at a temperature of 4.2 K. Because of the assumed lack of current carriers outside the channel we have no stationary current in the gate. On the other hand, however, the current instability is

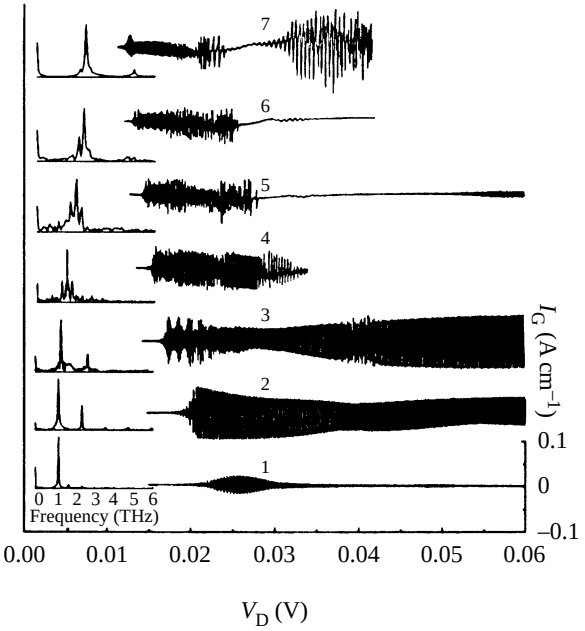

Fig. 4. Gate currents I_G versus drain potential V for gate potentials $V_G = -4$ mV (1), -8 mV (2), -25 mV (3), -50 mV (4), -75 mV (5), -100 mV (6), -125 mV (7). The Fourier analysis results are presented in the left-hand side insets. The I_G-current scale shown on the right-hand side is the same for all the curves.

developed apart the source—in the right part of the base, because the emitted from the source holes have to gain the NEM-section energy to become unstable. Therefore, most of the oscillation current flows through the gate and does not flow through the source. As a result, source current I_S is almost free of oscillations. A family of characteristics $I_S = I_S(V)$ for several values of V_G is shown in Fig. 3. We can see very small oscillations of I_S for negative gate voltages. They are much smaller than gate current oscillations shown for negative values of V_G in Fig. 4. The current oscillations are calculated by means of slow (quasiadiabatic) increasing V linearly with time: $V(t) = V(0) + V' \times t$, where V' is selected equal to 0.2 mV ps^{-1}. We obtain oscillation portraits for the whole interesting drain voltage range. (We are particularly interested in drain voltages $|V| < 36$ mV when the emission of optical phonons at low temperatures is impossible, and ballistic transport is quite realistic.) The high-frequency oscillation range narrows with increase in negative gate potential V_G. Simultaneously we can observe from the Fourier analysis (see the insets in Fig. 4) a substantial increase in oscillation frequencies: from $\approx$1.2 THz for $V_G = -4$ mV to $\approx$2.5 THz for $V_G = -125$ mV. Although these oscillations are noticeably nonlinear, they contain one or two key modes with the largest amplitudes. The highest frequencies of such modes occur for $V_G = -125$ mV.

4. Three forms of oscillatory regimes

In Fig. 4 the presented characteristics $I_G = I_G(V)$ (as well as characteristics of a drain current $I_D = I_{D1}(V)$ and $I_D = I_{D2}(V_G)$, which are not presented in this communication) demonstrate that regions of stable stationary regimes alternate with regions of oscillatory regimes. We observe three different forms of the oscillatory regimes listed below.

A. Oscillatory regimes, which take place approximately in the voltage ranges $V_C < V < V_K$ and

$|V_G| > 4$ mV. These regimes appear as results of development of NEM-instability. Oscillation frequencies rise monotonically with increase in $|V_G|$ (from 1.2 THz for $V_G = -4$ mV to 2.5 THz for $V_G = -125$ mV).

B. Oscillatory regimes, which take place in the extended drain voltage range (from $V = V_C$ to $V \sim 65$–70 mV) and in the restricted gate voltage range ($|V_G| = 8$–25 mV). These regimes are also initiated by NEM-instability. However, in this case voltages of saturation for both above-mentioned saturation forms are close to each other. Therefore, we have a single extended saturation region with NEM-holes as the predominating channel current carriers.

C. Oscillatory regimes, which take place for large values of $|V_G|$ (≥ 100 mV) and for values of V, which are between V_K and $\sim|V_G|$. This range is intermediate between sections of NEM-saturation and conventional FET-saturation. Two-stream instability considered in [2] for ballistic FET appears and develops in this range. Oscillation frequencies in the two-stream regime are substantially lower than frequencies in the NEM regime (for the same values of $|V_G|$). These frequencies also rise monotonically with an increase in $|V_G|$, and a drain voltage range of oscillation widens.

5. Conclusion

We have suggested introducing gates in the design of ballistic NEM generator and to transform it into a ballistic NEM FET. The gate potential allows us: (1) to switch oscillatory regimes and to control oscillation amplitudes, (2) to control oscillation frequencies in very wide ranges, and (3) to separate effectively loops of the stationary source current and the high-frequency gate current. As a result, we enhance functional abilities of the ballistic NEM generator.

Acknowledgements—This work was supported by NSF and JPL DFDR grants.

References

[1] A. A. Sukhanov, V. B. Sandomirskii, and Ya. Ya. Tkach, Sov. Phys. Semicond. **17**, 1378 (1983).
[2] V. V. Mantrov and A. A. Sukhanov, Sov. Phys. Semicond. **19**, 882 (1985).
[3] M. V. Nezlin, Sov. Phys. Uspekhi **11**, 608 (1971).
[4] V. I. Ryzhii, N. A. Bannov, and V. A. Fedirko, Sov. Phys. Semicond. **18**, 481 (1984).
[5] Z. S. Gribnikov and A. N. Korshak, Semiconductors **28**, 812 (1994).
[6] N. Z. Vagidov, Z. S. Gribnikov, and A. N. Korshak, JETP Lett. **61**, 38 (1995).
[7] Z. S. Gribnikov, N. Z. Vagidov, and A. N. Korshak, J. Appl. Phys. **80**, 5799 (1996).
[8] Z. S. Gribnikov, A. N. Korshak, N. Z. Vagidov, and V. V. Mitin, Int. J. Infrared Millim. Waves **20**, 213 (1999).